



Instruction Manual of an Ornithopter Flight Simulator

I-Wei Lee  and Sophie Armanini  

TUM School of Engineering and Design, Technical University of Munich

 iweilee@hotmail.com

 s.armanini@imperial.ac.uk

12 February, 2025

v.1.0.5

Abstract — This document is an instruction manual of the **OR**nithopter **F**light **S**imulator (ORFS), a flight simulator designed for a bird-like flapping-wing micro aerial vehicle (FWMAV) developed by Ornihobby [1]. It includes a concise overview of the modelling methodology, details the adjustable parameters available to users, offers instructions for running the simulator, and discusses the limitations.

1 Introduction

Flight simulators are widely used not only for training but also for testing. The design and development of an FWMAV rely heavily on trial-and-error approach. Simulation plays an important role in preventing costly hardware damage during test flights. ORFS is designed for bird-like FWMAVs, featuring two wings and a tail. However, its modular design allows users to adapt it to other types of FWMAVs seamlessly. The reference model is the FWMAV from Ornihobby, as shown in figure 1.



Figure 1: The FWMAV from Ornihobby with Wings flapping up and without Elevator and Rudder Deflection.

2 Modelling Approach

This section provides a brief overview of the modelling process, including wing motion, aerodynamics, and flight dynamics.

2.1 Wing Kinematics

The wing motion is described by its attitude, represented by the Euler angles Φ , Θ , and Ψ , which correspond to the rotation angle around x , y , and z axis, respectively.

2.2 Aerodynamics of the Wing

We assumed a quasi-steady aerodynamic model with blade element theory summarised by Sane [2] with constant air density and no disturbances at a trim condition, i.e., steady straight-level flight. According to the flapping mechanism of the FWMAV, our aerodynamic model contains four components: circulatory forces $d\mathbf{F}_{Cir}$, viscous forces $d\mathbf{F}_{Vis}$, rotational forces $d\mathbf{F}_{Rot}$ and the forces due to added-mass effect $d\mathbf{F}_{AM}$. The aerodynamic forces produced by each blade element $d\mathbf{F}_{Aero,Wing}$ are calculated as follows:

$$d\mathbf{F}_{Aero,Wing} = d\mathbf{F}_{Cir} + d\mathbf{F}_{Vis} + d\mathbf{F}_{Rot} + d\mathbf{F}_{AM} \quad (1)$$

Circulatory Force The circulatory force is commonly known as the lift for fixed-wing aircraft.

Viscous Force The viscous force is then the drag for the fixed-wing aircraft.

Rotational Force The rotational force is also known as the Kramer effect. Due to the rotations of the wing near the end of each stroke, additional circulations are needed to satisfy the Kutta condition. These additional circulations generate forces as well.

Added-Mass Effect Added mass describes the wing being subjected to a reaction force due to the air, which is accelerated by the wing acceleration. It is commonly seen in hydrodynamics but neglected in fixed-wing aerodynamics.

2.3 Aerodynamics of the Tail

The tail of the reference model acts like a ruddervator. It is driven by two servos, which allow it to flap up and down and rotate left and right. We assumed the forces and moments produced by the tail only depend on the angle of attack (AoA). Other effects, such as the side-slip angle, wing-tail interaction, etc., are neglected. Furthermore, with rudder deflection, the forces and the moments are rotated in the corresponding direction.

2.4 Dynamics

For the dynamic model we assumed that the Earth is flat and non-rotating, the gravitational acceleration g is constant, the FWMAV as a single symmetrical rigid body, its mass m and inertia matrix \mathbf{I} are constant over time. The states of the aircraft are $\mathbf{x} = [u, v, w, p, q, r, \phi, \theta, \psi, x, y, z]^T$, where u, v , and w are the body velocities; p, q , and r are the angular rates; ϕ, θ , and ψ are the Euler angles; and x, y , and z are the positions. The control inputs are $\mathbf{u} = [\delta_E, \delta_R, \delta_T]^T$, where δ_E is the elevator deflection, δ_R is the rudder deflection, and δ_T is the throttle. With Newton's second law, the theorem of the moment of momentum, and the previous assumptions, the Newton-Euler equations of the motion the FWMAV are:

$$\begin{aligned} \begin{bmatrix} \dot{u} \\ \dot{v} \\ \dot{w} \end{bmatrix} &= \frac{\mathbf{F}}{m} \cdot \begin{bmatrix} p \\ q \\ r \end{bmatrix} \times \begin{bmatrix} u \\ v \\ w \end{bmatrix} \\ \begin{bmatrix} \dot{p} \\ \dot{q} \\ \dot{r} \end{bmatrix} &= \frac{1}{\mathbf{I}} \cdot \left[\mathbf{M} - \begin{bmatrix} p \\ q \\ r \end{bmatrix} \times \left(\mathbf{I} \cdot \begin{bmatrix} p \\ q \\ r \end{bmatrix} \right) \right] \\ \begin{bmatrix} \dot{\phi} \\ \dot{\theta} \\ \dot{\psi} \end{bmatrix} &= \begin{bmatrix} 1 & \sin\phi\tan\theta & \cos\phi\tan\theta \\ 0 & \cos\phi & -\sin\phi \\ 0 & \frac{\sin\phi}{\cos\theta} & \frac{\cos\phi}{\cos\theta} \end{bmatrix} \cdot \begin{bmatrix} p \\ q \\ r \end{bmatrix} \\ \begin{bmatrix} \dot{x} \\ \dot{y} \\ \dot{z} \end{bmatrix} &= \begin{bmatrix} \cos\theta\cos\psi & \cos\theta\sin\psi & -\sin\theta \\ \sin\phi\sin\theta\cos\psi - \cos\phi\sin\psi & \sin\phi\sin\theta\sin\psi + \cos\phi\cos\psi & \sin\phi\cos\theta \\ \cos\phi\sin\theta\cos\psi + \sin\phi\sin\psi & \cos\phi\sin\theta\sin\psi - \sin\phi\cos\psi & \cos\phi\cos\theta \end{bmatrix} \cdot \begin{bmatrix} u \\ v \\ w \end{bmatrix} \end{aligned} \quad (2)$$

where F and M are the total forces and moments acting on the FWMAV, correspondingly.

3 Simulation Setup

This section covers the required parameters for running ORFS.

3.1 Time-Related Parameters

3.1.1 Total Time

The total time represents the total simulation time, which indicates the flight duration in the simulation. This is not equivalent to the actual time. To simulate in real-time, uncomment the `Simulation Pace` block before starting the simulation.

3.1.2 Time Step

ORFS is built with fixed time step in Simulink. The total time is discretised by the time step, which should be sufficiently small considering the Nyquist frequency. A recommended time step is 0.01 s.

3.2 Initial States

Aircraft dynamics is an initial value problem. Hence, initial conditions are required. These conditions include initial states and initial control inputs.

3.3 Control Inputs

As previously mentioned, the tail can rotate and flap up and down. The former corresponds the rudder input δ_R , while the latter represents the elevator input δ_E . To account for changes in flapping frequency, we borrowed the concept of throttle δ_T from fixed-wing aircraft. The flapping frequency is proportional to the rotational speed of the motor, and due to the linear relationship between the rotational speed and the motor voltage, the flapping frequency f is defined as follows:

$$f = \delta_T \cdot f_{max} \quad (3)$$

where f_{max} is the maximal flapping frequency.

There are three ways to generate the input signals: manual flight with a joystick or yoke, `Timetable` from MATLAB, and `Sources` from Simulink, such as a series combination of `Steps`.

3.3.1 Manual Flight

The benefit of manual flight is that the user does not need to know the actual values of the control variables. However, the drawback is that the user cannot precisely control the values of the variables. While flying manually, the `Joystick ID` must be checked first, and it is recommended to activate the `Simulation Pace` block. This block synchronises the simulation time with real time. The use of joysticks is designed analogously to the conventional aircraft control scenarios, i.e., pulling the joystick causes the aircraft to pitch up, joystick to the right initiates a right turn, and vice versa. The actual values of the control variables are linearly scaled between the minimal and the maximal values of the corresponding control variables. For further details, please refer to MathWorks® the help centre of `Pilot Joystick` block [3].

3.3.2 Timetable

The advantages of importing signal as **Timetable** is that the user can control the values of the control variables precisely, and the **Timetable** can be created with comma-separated values, Excel, and **linspace** functions. The disadvantages are that the values of the control variables must be assigned at each time step, which can lead to long and hard-to-track tables, and the user must understand the relationships between the signs of the values and the movements of the tail, for example, a positive elevator deflection means that the tail flaps down, leading the aircraft to pitch down; positive rudder deflection causes the tail rotates clockwise, resulting in a left turn, and vice versa. For further details, please refer to MathWorks® blogs by Rouleau [4, 5] and help centre of **From Spreadsheet** [6].

3.3.3 Sources

Last but not least, generating signals with **Sources** has the upsides that it is easy to use compared to the previous method, and it can provide accurate values of the control variables as well. Its downside is that as the number of signal changes increases, more **Sources** are required, which increases the complexity. Moreover, the user must have prior knowledge of the relationships between the signs of the values and the movements of the tail. For an abrupt change in signal, the **Sample time** property from **Sources** should be set to -1 , it is 0 by default. Otherwise, the signal changes linearly between the last value and the current value. For further details, please refer to MathWorks® help centre of **Sources** [7].

3.4 Wing Geometry

Wing geometry is required to calculate the chord length of the blade elements. To achieve this, the coordinates of the leading edge and trailing edge are essential. Ornihobby provides different wing configurations: 1.3 m standard wing, 1.4 m standard wing, and 1.4 m curved wing. The 1.5 m standard wing is no longer provided. The reference model has the 1.4 m standard wing.

3.5 Blade Element Number

The wing is discretised spanwise into equidistant wing strip, each of which can be consider as a two-dimensional (2D) airfoil. The blade element number n_{Blade} is defined as follow:

$$n_{Blade} = \frac{b}{dr} \quad (4)$$

where b is the wingspan and dr is the width of the wing strip. The blade element number should be at least larger than 20 in order to accurately prescribe the aerodynamics of the wing.

3.6 Aerodynamic Coefficients

The wide range of elevator deflection and the high AoA at the wingtip section due to the large wing span of the bird-like FWMAV both require a broad coverage of the AoA for the coefficients. Yet most research focuses only on the area up to stall. Therefore, it is hard to find suitable data for the coefficients.

3.6.1 Tail Coefficients

Initially, we used the coefficients from Guzmán et al. [8]. Yet their tail models are limited between $\pm 30^\circ$ of AoA, but the elevator deflection of FWMAV from Ornihobby can be larger than 30° . Hence, we ran Computational Fluid Dynamics (CFD) simulations to obtain the coefficients. The tail model from Guzmán et al. and our tail model behave similarly. The only difference is our model covers the AoA between $\pm 180^\circ$.

3.6.2 Wing Airfoil Coefficients

The airfoil of the wing is considered as flat plate since it is made from a thin membrane and carbon-fibre-reinforced plastic rods and plates. Three sets of coefficients are provided. If using alternative coefficient sets, please ensure they cover at least the range between $\pm 90^\circ$ of AoA.

Flat Plate The lift and drag coefficients of the flat plate are considered as triangular functions [9]. However, this set of coefficients cannot capture the stall and post-stall behaviours and is primarily derived from insect-scale flyers. To better represent the bird-like FWMAV we also take into account the coefficients from predatory birds, for instance, owls.

Flat Plate with CFD Simulation To address the issue of stall and post-stall behaviour, we conducted 2D CFD simulations. The chord length of the flat plate is set to the mean aerodynamic chord length of the wing. However, with this set of coefficients, the FWMAV is unable to maintain its altitude, even with the maximal throttle setting.

NACA 0009 Thin, symmetrical NACA four-digit airfoil, such as NACA 0009, are commonly used as flat plates. However, its maximal lift coefficient is insufficient and the maximal drag coefficient is excessively large [10], preventing the FWMAV from becoming airborne.

4 Known Issue

The main issue is the lack of flight tests, meaning the actual values of the parameters may differ. However, we considered several studies on similar drones, the same FWMAV with different wing and tail configurations, earlier versions of the FWMVA from OrniHobby, and biological data from large-scale flyers. Feel free to reach out to us for relevant papers.

4.1 Wing Kinematics

The wing is assumed as rigid body with spanwise linear twist, i.e., the maximal and minimum twisting angles at wing tip and without wing twist at wing root. These maximal and minimal twisting angles are measured with the wing positioned horizontally to the ground, where the wing undergoes passive twisting due to gravitational forces. Although birds do not typically rotate their wings actively like insects, the CFRP rod arrangement of the reference model causes the outer section of the wing to rotate passively.

4.2 Aerodynamic Coefficients

The rotational coefficient in section 2.2 is derived from the research of Dickinson et al. [11] and Sane and Dickinson [12]. Experiments are required to adapt the rotational coefficient to large-scale FWMAVs. For the added-mass effect, the model needs to be improved to capture the acceleration of each wing strip more precisely.

4.3 Unsteady Aerodynamics

Several unsteady aerodynamic effects are neglected, including wing-wake interaction, especially during slow flight, and wing-tail interaction.

4.4 Dynamics

As mentioned in section 2.4, the Euler angles ϕ , θ , and ψ are used as attitude states. In extreme flight manoeuvres, such as perching, birds pitch up drastically and approach a near vertical position just before landing. At pitch angle θ of 90° causes singularities and leads to failure in simulation.

References

- [1] Ornihobby. www.ornihobby.com (accessed May. 02, 2023).
- [2] S. P. Sane, “The Aerodynamics of Insect Flight,” *The Journal of Experimental Biology*, vol. 206, no. 23, 2003.
- [3] MathWorks® Help Center, “Pilot Joystick.” <https://www.mathworks.com/help/aeroblks/pilotjoystick.html> (accessed May. 02, 2023).
- [4] G. Rouleau, “Using Discrete Data as an input to your Simulink model.” <https://blogs.mathworks.com/simulink/2012/02/09/using-discrete-data-as-an-input-to-your-simulink-model/> (accessed May. 02, 2023).
- [5] G. Rouleau, “Loading Signals in Timetable Format.” https://blogs.mathworks.com/simulink/2019/08/06/loading-signals-in-timetable-format/?s_tid=prof_contriblnk (accessed May. 02, 2023).
- [6] MathWorks® Help Center, “From Spreadsheet.” <https://www.mathworks.com/help/simulink/slref/fromspreadsheet.html> (accessed May. 02, 2023).
- [7] MathWorks® Help Center, “Sources.” <https://www.mathworks.com/help/simulink/sources.html> (accessed May. 02, 2023).
- [8] M. Guzmán, C. R. Páez, F. J. Maldonado, R. Zufferey, J. Tormo-Barbero, J. Acosta, and A. Ollero, “Design and Comparison of Tails for Bird-Scale Flapping-wing Robots,” in *2021 IEEE/RSJ International Conference on Intelligent Robots and Systems (IROS)*, pp. 6358–6365, 2021.
- [9] H. E. Taha, M. R. Hajj, and P. S. Beran, “State-space representation of the unsteady aerodynamics of flapping flight,” *Aerospace Science and Technology*, vol. 34, pp. 1–11, 2014.
- [10] R. E. Sheldahl and P. C. Klimas, “Aerodynamic Characteristics of Seven Symmetrical Airfoil Sections through 180-Degree Angle of Attack for Use in Aerodynamic Analysis of Vertical Axis Wind Turbines,” report, United States Department of Energy, 1981.
- [11] M. H. Dickinson, F.-O. Lehmann, and S. P. Sane, “Wing Rotation and the Aerodynamic Basis of Insect Flight,” *Science*, vol. 284, no. 5422, pp. 1954–1960, 1999.
- [12] S. Sane and M. Dickinson, “The aerodynamic effects of wing rotation and a revised quasi-steady model of flapping flight,” *The Journal of Experimental Biology*, vol. 205, pp. 1087–1096, 2002.